

QGSJET-II: towards reliable description of very high energy hadronic interactions

S. Ostapchenko^{a,b*}[†]

^aInstitut für Experimentelle Kernphysik, University of Karlsruhe, 76021 Karlsruhe, Germany

^bD.V. Skobeltsyn Institute of Nuclear Physics, Moscow State University, 119992 Moscow, Russia

Since a number of years the QGSJET model has been successfully used by different groups in the field of high energy cosmic rays. Current work is devoted to the first general update of the model. The key improvement is connected to an account for non-linear interaction effects which are of crucial importance for reliable model extrapolation into ultra-high energy domain. The proposed formalism allows to obtain a consistent description of hadron-hadron cross sections and hadron structure functions and to treat non-linear effects explicitly in individual hadronic and nuclear collisions. Other ameliorations concern the treatment of low mass diffraction, employment of realistic nuclear density profiles, and re-calibration of model parameters using a wider set of accelerator data.

1. INTRODUCTION

All experimental studies of cosmic rays (CR) of energies above 10^{14} eV are based on an indirect method: properties of the primary particles are reconstructed on the basis of measured characteristics of extensive air showers (EAS), induced by them in the atmosphere. The quality of such a reconstruction depends strongly on the present understanding of complicated EAS physics, especially concerning its backbone – hadron cascade process. By consequence, Monte Carlo (MC) modelization of high energy interactions plays an important role in CR investigations.

Among other hadronic MC generators, employed in EAS simulations, the QGSJET model [1,2,3] has been extensively used in the field, being applied for projecting new experiments, analyzing and interpreting data of various experimental installations. Being originally based on the Quark-Gluon String model [4] picture of high energy interactions, it has been generalized to treat nucleus-nucleus interactions [1] and semihard processes, using so-called "semihard Pomeron" ap-

proach [2,3] (see also [5,6,7]).

Current work is devoted to another important development of the scheme - a treatment of non-linear interaction effects. The latter are described by so-called enhanced Pomeron diagrams [8,9,10,11] and proved to be of extreme importance for a correct treatment of very high energy hadronic interactions. The approach proposed here is based on the assumption that corresponding effects are dominated by "soft" (low momentum transfer) partonic processes [12,13]. For the first time, essential enhanced contributions have been re-summed to all orders, both for so-called uncut (elastic scattering) diagrams and for various unitarity cuts of those diagrams, corresponding to particular final states of the interaction [15]. Based on the obtained solutions, a new hadronic interaction model QGSJET-II has been developed, explicitly treating the corresponding effects in individual hadronic (nuclear) collisions.

2. QGSJET MODEL

QGSJET model treats hadronic and nuclear collisions in the framework of Gribov's reggeon approach [8,9] – as multiple scattering processes – Fig. 1, where individual scattering contributions are described phenomenologically as Pomeron ex-

*Now at Forschungszentrum Karlsruhe, Institut für Kernphysik, 76021 Karlsruhe, Germany.

[†]This work has been supported in part by the German Ministry for Education and Research (BMBF, Grant 05 CU1VK1/9).

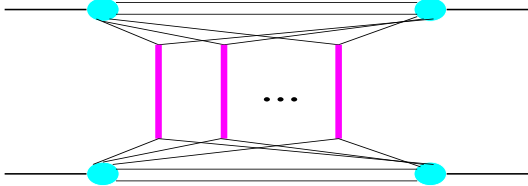


Figure 1. A general multi-Pomeron contribution to hadron-hadron scattering amplitude; elementary scattering processes (vertical thick lines) are described as Pomeron exchanges.

changes. The latter correspond to microscopic parton (quark and gluon) cascades, which mediate the interaction between the projectile and the target hadron, and consist of two parts: "soft" and "semihard" Pomerons – Fig. 2. The former, described by the corresponding eikonal $\chi_P(s, b)$, represents a purely "soft" cascade of partons of low virtualities $|q^2| < Q_0^2$, with Q_0^2 being some chosen virtuality cutoff, whereas the latter, with the eikonal $\chi_{sh}(s, b)$, corresponds to a cascade which at least partly develops in a high virtuality ($|q^2| > Q_0^2$) region and is typically represented by a piece of QCD ladder sandwiched between two soft Pomerons [2,3,5].

Calculating various unitarity cuts of elastic scattering diagrams of Fig. 1 according to Abramovskii-Gribov-Kancheli (AGK) cutting rules [14] one can obtain expressions for total and inelastic cross sections as well as for relative probabilities of particular interaction configurations, e.g., for a given number of elementary inelastic processes ("cut" Pomerons), all being expressed via the total eikonal $\chi_{tot}(s, b) = \chi_P(s, b) + \chi_{sh}(s, b)$. This allows in turn to perform a modeling of hadronic (nuclear) interactions via a MC method [3]: starting from sampling a particular configuration, at some impact parameter b (nucleon coordinates) and with some numbers of "cut" soft and semihard Pomerons; performing energy-momentum sharing between elementary inelastic interactions and between soft and hard partonic processes; simulating explicitly perturbative parton cascades; and finishing with a hadronization of strings stretched between con-

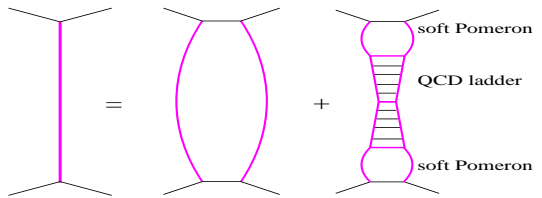


Figure 2. A "general Pomeron" (l.h.s.) consists of the "soft" and "semihard" Pomerons - correspondingly the 1st and the 2nd contributions on the r.h.s.

stituent partons (Pomeron "ends") of the projectile and the target, and between final on-shell partons resulted from the QCD cascades above.

3. NON-LINEAR EFFECTS

The above-described scheme is based on the assumption that individual parton cascades, described as Pomeron exchanges, proceed independently of each other. This condition cease to be valid in the limit of high energies and small impact parameters of the interaction, where a large number of elementary scattering processes occurs and corresponding underlying parton cascades strongly overlap and interact with each other, the effects being described as Pomeron-Pomeron interactions [8,9,10,11]. We make a basic assumption that the latter are dominated by partonic processes at comparatively low virtuality scale, $|q^2| < Q_0^2$ [12,13].

Then multi-Pomeron vertexes involve only interactions between soft Pomerons or between soft "ends" of semihard Pomerons – Fig. 3. At not

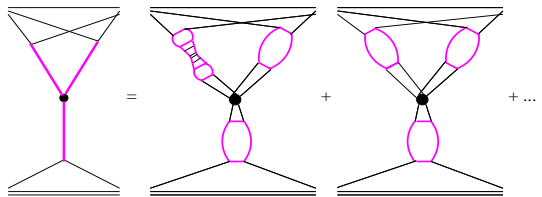


Figure 3. Contributions to the triple-Pomeron vertex from interactions between soft and semihard Pomerons.

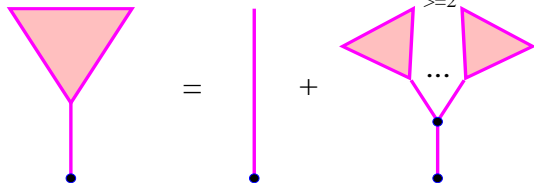


Figure 4. Recursive equation for a “fan” diagram contribution (constituent partons not shown).

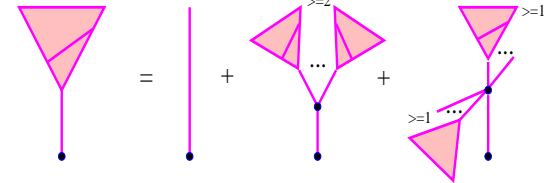


Figure 5. Recursive equation for a “generalized fan” contribution.

too high energies it is sufficient to consider the contributions with just one vertex of that kind. However, with the energy increasing one has to re-sum all essential higher order corrections.

We start from calculating the “fan” diagram contribution, given by a recursive graphical equation of Fig. 4. In addition, we define a “generalized fan” contribution as shown in Fig. 5; the latter includes also vertexes with both “fans” connected to the projectile and ones connected to the target. Then, neglecting subdominant contributions of Pomeron loops, the final result for hadron-hadron interaction eikonal can be represented in the graphical form as shown in Fig. 6 [15]. Correspondingly, hadron-hadron elastic scattering amplitude is now given by the sum of diagrams of Fig. 1, with simple Pomeron exchanges (vertical lines in the Figure) being replaced by the full set of diagrams of Fig. 6.

To calculate probabilities of various interaction configurations one has to consider all unitarity cuts of the diagrams of Fig. 6 and to re-sum contributions of cuts of certain types. The results obtained have been used to construct a new MC procedure which allows to sample explicitly interaction events of complicated topologies and to account for all screening corrections for particular cut Pomeron configurations [15].

The treatment of hadron-nucleus and nucleus-nucleus collisions is realized in a similar way, without introducing any additional parameters. There, an important aspect is that different Pomerons belonging to the same enhanced graph may be coupled to different nucleons of the projectile (target). As a consequence, non-linear screening effects are stronger in nuclear case; in

particular, this leads to a violation of the superposition picture for nucleus-induced air showers even for average EAS characteristics [16].

4. DISCUSSION

Apart from the basic development, described above, the new model included realistic nuclear density parameterizations, individually for each nucleus [17], and more reliable two-component low mass diffraction treatment [1]. All model parameters have been re-calibrated using a wider set of accelerator data. The obtained results for hadron-nucleus interactions and for EAS characteristics will be presented elsewhere [16]. Here we illustrate the importance of Pomeron-Pomeron interactions calculating total proton-proton cross section both with and without enhanced diagram contributions – Fig. 7. Correspondingly, proton structure function (SF) $F_2(x, Q_0^2)$, $Q_0^2 = 2 \text{ GeV}^2$, again calculated with and without enhanced diagrams, is shown in Fig. 8 (charm contribution not included).

It is important to note that the contribution of semihard processes to the interaction eikonal can no longer be expressed in the usual factorized form, which was assumed so far in all hadronic MC models. The non-factorizable contributions arise from graphs where at least one Pomeron is exchanged in parallel to the parton hard process, with the simplest example given by the 1st diagram on the r.h.s. in Fig. 3. At the same moment, due to the AGK cancellations [14] such diagrams give zero contribution to inclusive high- p_t jet spectra and the scheme preserves the QCD factorization picture for inclusive jet production.

In conclusion, the new model is based on a

$$\chi_{\text{tot}} = \left| + \begin{array}{c} \text{triangle} \\ \diagup \quad \diagdown \\ \bullet \\ \diagdown \quad \diagup \\ \text{triangle} \end{array} \begin{array}{c} \geq 1 \\ \dots \\ \geq 1 \end{array} - 1/2 \left(\begin{array}{c} \text{triangle} \\ \diagup \quad \diagdown \\ \bullet \\ \diagdown \quad \diagup \\ \text{triangle} \end{array} \begin{array}{c} \geq 1 \\ \dots \\ \geq 0 \end{array} - \begin{array}{c} \text{triangle} \\ \diagup \quad \diagdown \\ \bullet \\ \diagdown \quad \diagup \\ \text{triangle} \end{array} \begin{array}{c} >= 2 \\ \dots \\ >= 2 \end{array} - \begin{array}{c} \text{triangle} \\ \diagup \quad \diagdown \\ \bullet \\ \diagdown \quad \diagup \\ \text{triangle} \end{array} \begin{array}{c} >= 2 \\ \dots \\ >= 2 \end{array} - \begin{array}{c} \text{triangle} \\ \diagup \quad \diagdown \\ \bullet \\ \diagdown \quad \diagup \\ \text{triangle} \end{array} \begin{array}{c} = 1 \\ \dots \\ >= 2 \end{array} \right) - 1/2 \left(\begin{array}{c} \text{triangle} \\ \diagup \quad \diagdown \\ \bullet \\ \diagdown \quad \diagup \\ \text{triangle} \end{array} \begin{array}{c} >= 2 \\ \dots \\ >= 2 \end{array} \end{array} \right) \right|$$

Figure 6. Total hadron-hadron interaction eikonal, including enhanced diagram contributions.

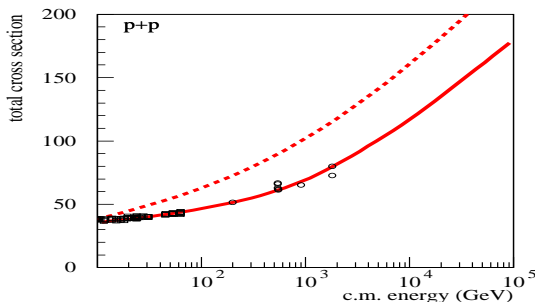


Figure 7. Total pp cross section calculated with (full curve) and without (dashed curve) enhanced diagram contributions. The data are from [18].

consistent treatment of enhanced Pomeron diagrams and allows to get agreement between the measured hadronic cross sections and structure functions and to account for non-linear interaction effects explicitly in individual hadronic and nuclear collisions.

REFERENCES

1. N.N. Kalmykov and S.S. Ostapchenko, Phys. Atom. Nucl. 56 (1993) 346.
2. N.N. Kalmykov *et al.*, Bull. Russ. Acad. Sci. Phys. 58 (1994) 1966.
3. N.N. Kalmykov *et al.*, Nucl. Phys. Proc. Suppl. 52B (1997) 17.
4. A.B. Kaidalov and K.A. Ter-Martirosian, Phys. Lett. B117 (1982) 247.
5. S. Ostapchenko *et al.*, Nucl. Phys. Proc. Suppl. 52B (1997) 3.
6. H.J. Drescher *et al.*, J. Phys. G: Nucl. Part. Phys. 25 (1999) L91.
7. S. Ostapchenko *et al.*, J. Phys. G: Nucl. Part. Phys. 28 (2002) 2597.

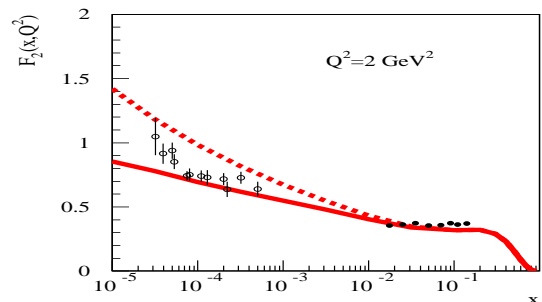


Figure 8. Proton SF F_2 calculated with (full curve) and without (dashed curve) enhanced diagram contributions. The data are from [19,20,21].

8. V.N. Gribov, Sov. Phys. JETP 26 (1968) 414.
9. V.N. Gribov, Sov. Phys. JETP 29 (1969) 483.
10. O. Kancheli, JETP Lett. 18 (1973) 465.
11. J. L. Cardy, Nucl. Phys. B75 (1974) 413.
12. H.J. Drescher *et al.*, Phys. Rep. 350 (2001) 93.
13. S. Ostapchenko, J. Phys. G: Nucl. Part. Phys. 29 (2003) 831.
14. V.A. Abramovskii *et al.*, Sov. J. Nucl. Phys. 18 (1974) 308.
15. S. Ostapchenko, in preparation.
16. S. Ostapchenko, Nucl. Phys. Proc. Suppl. B (2005), these proceedings.
17. N.N. Kalmykov *et al.*, Proc. 26th Int. Cosmic Ray Conf. (Salt Lake City), v.1, p.419 (1999).
18. C. Caso *et al.*, Eur. Phys. J. C3 (1998) 1.
19. S. Aid *et al.*, H1 Collaboration, Nucl. Phys. B470 (1996) 3.
20. M. Derrick *et al.*, ZEUS Collaboration, Z. Phys. C72 (1996) 399.
21. M. Arneodo *et al.*, NMC Collaboration, Phys. Lett. B364 (1995) 107.